Fabrication of 3D-Printed Flow Cell Biosensor for Pathogenic Escherichia Coli Bacteria Detection

Muhammad Fadzlisyam Redzuan[1], Irfan Danial Ismadi[1], Muhammad Fakhrullah Mohamad Azmi[1], Izzah Afifah Ibrahim[1], Mohd Ifwat Mohd Ghazali[1], Nurul Azmawati Mohamed[2], Nizam Tamchek[3], & Shahino Mah Abdullah[1*]

[1]*Faculty Science and Technology, Universiti Sains Islam Malaysia, 71800, Nilai, Negeri Sembilan, Malaysia*

[2]*Faculty of Medicine & Health Sciences, Universiti Sains Islam Malaysia, 71800, Nilai, Negeri Sembilan, Malaysia*

[3]*Department of Physics, Universiti Putra Malaysia, 43400, Serdang, Selangor, Malaysia*

Abstract
This research seeks to develop an innovative 3D-printed biosensor for the rapid and accurate detection of Escherichia coli (E. coli) bacteria in water samples. The proposed biosensor will incorporate a flow cell design, which allows continuous monitoring and efficient detection of E. coli in real-time. The sensor will be fabricated using conductive polymer-based materials integrated with specific biological recognition elements to ensure high sensitivity and specificity. The 3D printing technology will be utilized to create a precise and reproducible flow cell structure, optimizing the sensor's functionality and scalability. The research will proceed through several key phases: designing and simulating the flow cell structure, selecting and functionalizing the sensing materials, fabricating the biosensor using 3D printing techniques, and conducting extensive testing with water samples containing various concentrations of E. coli. This research will establish a foundation for future advancements in portable and effective biosensing devices for early detection of bacterial contamination.

Keywords: *Escherichia Coli; Biosensor; Flow Cell; 3D printing*

1.0 Introduction

Traditional methods for detecting E. coli contamination, such as culture-based techniques and polymerase chain reaction (PCR), while effective, are time-consuming, labor-intensive, and require specialized laboratory equipment. These limitations create a demand for more efficient, portable, and real-time detection methods. Biosensors offer a promising solution, providing the capability to detect E. coli rapidly and accurately without the need for extensive sample preparation or sophisticated instrumentation. The development of biosensors for E. coli detection addresses several critical needs involving speed, portability, sensitivity, and cost-effectiveness [1]. In this case, rapid detection can prevent the spread of contamination and enable timely interventions. Field-deployable sensors allow on-site testing in various environments, from food processing plants to remote water sources. High sensitivity ensures the detection of low bacterial concentrations, while specificity ensures that the sensor targets E. coli strains accurately without cross-reacting with other microorganisms.

Flow cell biosensors based on electrochemical structure have emerged as a superior design for detecting bacterial contamination Fig. 1. The flow cell structure offers several advantages that include continuous monitoring, enhanced sensitivity, improved response time, and reduced fouling [2,3]. The flow cell design allows for the continuous flow of samples through the sensor, enabling real-time monitoring and immediate detection of contaminants [4]. The continuous flow ensures that fresh samples are constantly exposed to the sensing elements, increasing the likelihood of detecting bacteria even at low concentrations.

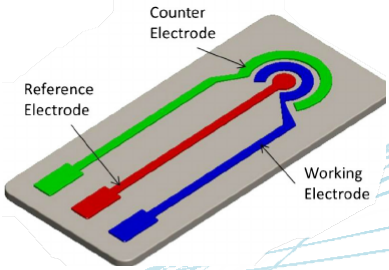

Fig. 1. Basic construction of electrochemical flow cell sensor

This research will leverage 3D printing technology in biosensor production Fig. 2. 3D printing allows for the precise and reproducible creation of complex sensor structures that would be challenging to produce using traditional manufacturing methods [5]. Key benefits of using 3D printing for biosensor production include customization, scalability, precision, and material versatility. In this case, 3D printing enables the design and production of biosensors tailored to specific applications and requirements. 3D printing supports a wide range of materials, including biocompatible polymers and conductive materials, essential for the construction of functional biosensors.

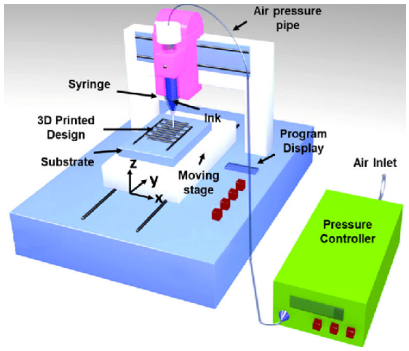

Fig. 2. Sensor fabrication via 3D printing technique

Potassium chloride (KCl) is the most widely used supporting electrolyte solution for application in cyclic voltammetry (CV) experiments because of high aqueous solubility and good conductor [6], providing optimum ionic strength and enhancing solution conductivity. This minimizes uncompensated resistance and leads to greater accuracy and reproducibility in electrochemical measurement. In addition to that, chloride ions in KCl are able to stabilize some metal cations via complex formation, influencing their electrochemical reactions.

Nickel (II) phthalocyanine-tetrasulfonic acid tetrasodium salt (NiTsPc) is a water-soluble chemical having a stable planar structure Fig. 3. Its four sulfonate groups allow it to dissolve in water, making it suitable for a variety of applications. NiTsPc is commonly used to construct nanostructures such as thin films with layer-by-layer (LbL) assembly. This experiment will utilize a combined solution of Potassium Chloride (KCl) and nickel (II) phthalocyanine-tetrasulfonic acid tetrasodium salt (NiTsPc) as the water sample for cyclic voltammetry (CV) experiments and biosensor testing.

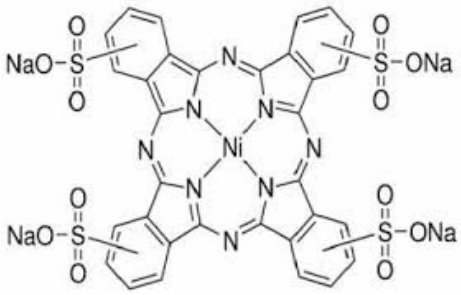

Fig. 3. Molecular structures of NiTsPc

2.0 Methodology

2.1 Design and selection of sensing materials

The initial phase of the research involves the conceptualization and optimization of the 3D-printed flow cell biosensor's design. This begins with an extensive literature review to understand the current advancements and limitations in biosensor technology, particularly focusing on flow cell designs. Using computer-aided design (CAD) software, detailed models of the flow cell structure will be created, incorporating microfluidic channels and sensor integration points to facilitate optimal fluid dynamics and bacterial interaction Fig. 4 [7,8].

The second phase focuses on the selection and functionalization of conductive polymer-based materials to be used in the biosensor. The process begins by identifying and testing various conductive polymers suitable for 3D printing and biosensing applications. Fluid dynamics simulations will be conducted to analyse and refine the flow patterns, shear stress, and bacteria transport mechanisms within the flow cell. Initial prototypes will be fabricated using 3D printing technology to test the feasibility and practicality of the design. The outcome of this phase will be a validated and optimized flow cell structure that ensures efficient fluid dynamics, setting a solid foundation for the subsequent phases of biosensor development.

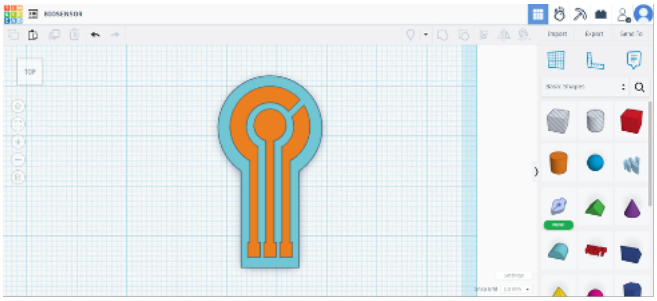

Fig. 4. Schematic of the 3D-printed flow cell biosensor's design

2.2 Setup for the cyclic voltammetry (CV) testing

This phase began with the preparation of the cyclic voltammetry (CV) setup to evaluate its performance on the water samples Fig. 5. The Analog Device ADALM1000 was used to demonstrate the relationship between current, voltage, and impedance (including resistance, inductance, and capacitance). When connected to a laptop or tablet, the ADALM1000 functioned as a personal portable laboratory [9]. Pixelpulse2, an open-source program, provided a user interface for visualizing and adjusting signals while analyzing systems connected to the device.

The CV setup included three different electrode materials: 1) platinum (Pt) as the counter electrode, which was connected to the GND of the ADALM1000, 2) graphite (Gr) as the working electrode, which was connected to the CHA of the ADALM1000, and 3) silver chloride (AgCl) as the reference electrode, which was connected to the CHB of the ADALM1000. For the preparation of the water sample used to systematically evaluate the CV's performance, the experiment utilized two solutions consisting of: 1) 40 mL of 3M KCl combined with 3 mL of 0.1M KCl + 0.5 mg/mL of NiTsPc, and 2) 40 mL of 3M KCl combined with 6 mL of 0.1M KCl + 0.5 mg/mL of NiTsPc.

The CV measurements were conducted over 3 complete cycles to ensure consistency and repeatability of the electrochemical response. No specific scan rate was defined during the experiment, as the ADALM1000 and Pixelpulse2 interface operated based on time-domain sampling rather than conventional potentiostat scan rate settings. The sampling rate was set to 1000 samples per second to capture detailed current and voltage fluctuations during each cycle. These parameters were chosen to balance data resolution with system stability and processing efficiency.

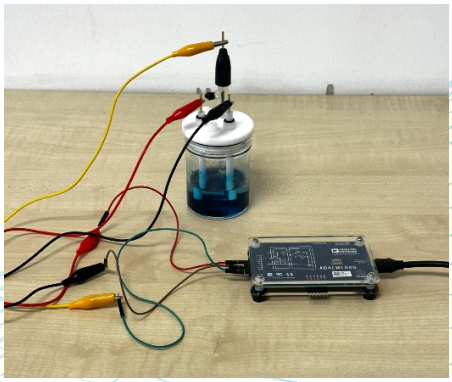

Fig. 5. Setup for the cyclic voltammetry (CV) testing

2.3 *Setup for the 3D-printed flow cell biosensor testing*

The experiment continued with the preparation of the 3D-printed flow cell biosensor setup to evaluate its performance on the water samples Fig. 6. In this phase, only the CV component was replaced with the biosensor, while the other devices remained the same for data evaluation.

The biosensor also contained three different electrodes: 1) the counter electrode was connected to the GND of the ADALM1000, 2) the working electrode was connected to the CHA of the ADALM1000, and 3) the reference electrode was connected to the CHB of the ADALM1000. The biosensor was tested by before and after applying a solution of 0.1M KCl + 0.5 mg/mL of NiTsPc onto its conductive surface to obtain the readings.

The biosensor's performance was rigorously compared with conventional detection methods to validate its effectiveness and highlight its advantages. This phase aimed to generate comprehensive data demonstrating the biosensor's high sensitivity, specificity, and reliability in detecting E. coli.

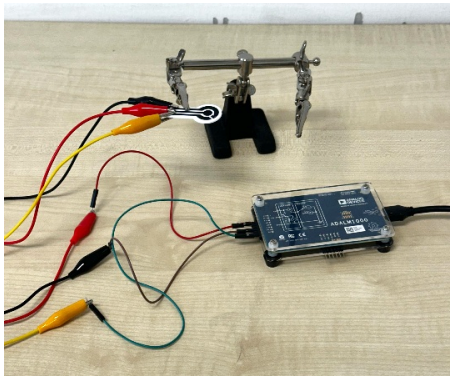

Fig. 6. Setup for the 3D-printed flow cell biosensor testing

3.0 Result and discussion

3.1 Fabrication of the biosensor using 3D printing

The research is centered on the actual fabrication of the 3D-printed flow cell biosensor using advanced 3D printing techniques Fig. 7 [10]. High-resolution Bambu Lab A1 mini 3D printers will be employed to fabricate the optimized flow cell structure, ensuring precise replication of the design developed in the first phase [11]. The integration of the functionalized sensing materials into the 3D-printed flow cell structure is a critical step, requiring precise alignment and secure attachment to maintain the sensor's functionality [12]. The complete assembly of the biosensor will also include necessary electronic components for signal transduction and data acquisition. Throughout this process, rigorous quality

control tests will be conducted to verify the structural integrity and functionality of the biosensor components. This phase will culminate in a fully assembled and functional 3D-printed flow cell biosensor, poised for performance evaluation and testing. The use of 3D printing technology not only ensures high precision and customization but also offers a cost-effective and scalable approach to biosensor production [13].

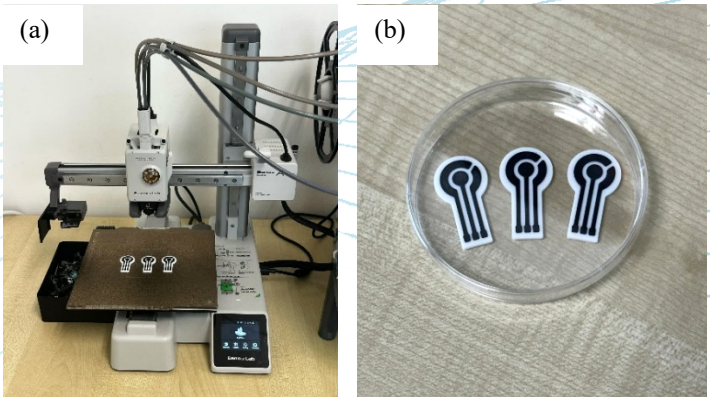

Fig. 7. (a) The advanced 3D printing techniques; (b) the actual fabrication of the 3D-printed flow cell biosensor

3.2 Testing on the cyclic voltammetry (CV)

The CV graph illustrated the response of how the current changed as the voltage was scanned in both the forward and reverse directions Fig. 8. The solution for this experiment was prepared using 40 mL of 3M KCl combined with 3 mL of 0.1M KCl + 0.5 mg/mL of NiTsPc. The results indicated variations in current as the voltage was applied in both directions. It showed that there were no clear peaks of oxidation and reduction available because the electrolyte solution might be insufficient at low concentration. Despite these fluctuations, the graph demonstrated the ability to form a distinguishable cyclic voltammetry. The current (A) ranged from approximately -0.035 to 0.04 A, while the voltage (V) varied between 0 and 3 V.

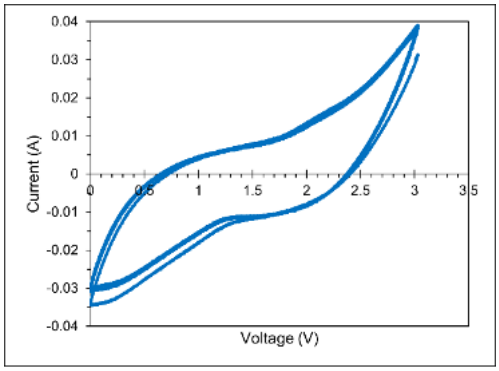

Fig. 8. CV's graph of 40 mL of 3M KCl with 3 mL of 0.1M KCl + 0.5 mg/mL of NiTsPc

This part showed the typical shape with an oxidation (anodic) and reduction (cathodic) peak illustrating the electroactivity of the system Fig. 9. Red lines showed the slope of different regions with response to the change in the current, and green arrows showed the voltage readings for oxidation was 2.2 V and reduction was 0.9 V. The solution for this experiment was prepared with 40 mL of 3M KCl with 6 mL of 0.1M KCl + 0.5 mg/mL of NiTsPc, and this could have impacted the electron transfer process and enhanced the electroactivity of the sensor. The current (A) ranged from approximately -0.027 to 0.03 A, while the voltage (V) varied between 0 and 3 V. The shape of the cyclic voltammetry

showed excellent electron transfer characteristics, as reflected by the relatively symmetrical oxidation and reduction peaks.

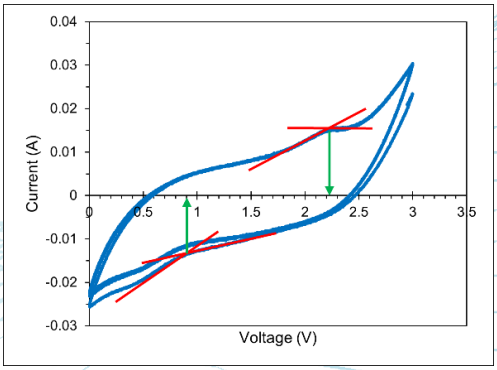

Fig. 9. CV's graph of 40 mL of 3M KCl with 6 mL of 0.1M KCl + 0.5 mg/mL of NiTsPc

To clearly compare the performance under both conditions, Table 1 summarizes the key observations from each CV test:

Solution Composition	Current Range (A)	Voltage Range (V)	Redox Peaks
40 mL 3M KCl + 3 mL 0.1M KCl + 0.5 mg/mL NiTsPc	-0.035 to 0.04	0 – 3	Not clearly visible
40 mL 3M KCl + 6 mL 0.1M KCl + 0.5 mg/mL NiTsPc	-0.027 to 0.03	0 – 3	Oxidation at 2.2 V, Reduction at 0.9 V

This comparison reinforces the importance of optimal electrolyte concentration in achieving effective redox activity and highlights the potential of the CV setup in future electrochemical sensing applications.

3.3 Testing on the 3D-printed flow cell biosensor

As stated in the method, the 3D-printed flow cell biosensor was tested before and after the electrolyte solution was applied. Fig. 10 displayed the graph obtained when the biosensor was tested without any solution. The result showed that the voltage (V) ranged from 0 to 0.5 V, remaining nearly constant at Channel B across each cycle.

Fig. 10. Biosensor's graph without any solution

Next, the solution for this experiment was prepared using 0.1M KCl + 0.5 mg/mL of NiTsPc, then applied to the biosensor to obtain the graph Fig. 11. The results showed that the voltage (V) ranged from 0 to 1.4 V. A clear change was detected as the peaks increased, indicating that the biosensor exhibited conductive capability in detecting the solution.

Fig. 11. Biosensor's graph with the solution of 0.1M KCl + 0.5 mg/mL of NiTsPc

To provide a clearer comparison of performance, Table 2 summarizes the key voltage responses observed before and after the electrolyte solution was introduced:

Condition	Voltage Range (V)	Peak Presence	Conductive Response
Before solution application	0 – 0.5	No peaks	Minimal
After solution application	0 – 1.4	Clear peaks	Significant

This comparison highlights the sensitivity of the 3D-printed biosensor to the electrolyte solution, suggesting its potential applicability in detecting analytes such as E. coli in future work.

4.0 Conclusion

The CV experiment achieved voltage readings of 2.2 V for oxidation and 0.9 V for reduction. The results indicated that the minimum electrolyte concentration required to obtain distinct oxidation and reduction peaks were 40 mL of 3M KCl mixed with 6 mL of 0.1M KCl + 0.5 mg/mL of NiTsPc. When a lower concentration was used, no significant reaction was observed. In the biosensing experiment, the results demonstrated that the fabricated 3D-printed biosensor generated a response upon contact with electrolyte solutions. It could be concluded that the fabrication of the 3D-printed flow cell biosensor using advanced 3D printing techniques achieved early success, as it was a low-cost, biodegradable, and mass-producible alternative to conventional methods. This suggests that the biosensor could serve as a practical alternative for detecting various water samples in real-life applications such as detecting E. coli or any bacterial disease. Although direct testing with E. coli samples has not yet been conducted, the experimental methods and preliminary results confirm the biosensor's functional responsiveness to electrolytic changes, indicating strong potential for bacterial detection. These findings lay the groundwork for future studies, where the biosensor will be further validated using real E. coli samples to confirm its specificity and sensitivity. Therefore, the current experiments provide a solid foundational approach toward developing an effective tool for microbial water quality monitoring.

Acknowledgement

This research was supported by the Ministry of Higher Education, Malaysia under the Fundamental Research Grant Scheme (FRGS/1/2024/STG07/USIM/02/1). The research was also funded by Universiti Sains Islam Malaysia under USIM Research Grant (PPPI/USIM/FST/USIM/112623).

References

[1] Y. Huang, Z. Su, W. Li, and J. Ren, (2022) "Recent Progresses on Biosensors for Escherichia coli Detection," *Food Anal Methods*, vol. 15, no. 2, pp. 338–366, doi: 10.1007/S12161-021-02129-7.

[2] S. Damiati and B. Schuster, (2020) "Electrochemical Biosensors Based on S-Layer Proteins," *Sensors 2020, Vol. 20, Page 1721*, vol. 20, no. 6, p. 1721, doi: 10.3390/S20061721.

[3] M. M. Ovhal, N. Kumar, and J. W. Kang, (2020) "3D direct ink writing fabrication of high-performance all-solid-state micro-supercapacitors," *Molecular Crystals and Liquid Crystals*, vol. 705, no. 1, pp. 105–111, doi: 10.1080/15421406.2020.1743426.

[4] R. Domingo-Roca *et al.*, (2023) "Rapid assessment of antibiotic susceptibility using a fully 3D-printed impedance-based biosensor," *Biosens Bioelectron X*, vol. 13, p. 100308, doi: 10.1016/J.BIOSX.2023.100308.

[5] I. G. Siller, J. A. Preuss, K. Urmann, M. R. Hoffmann, T. Scheper, and J. Bahnemann, (2020) "3D-Printed Flow Cells for Aptamer-Based Impedimetric Detection of E. coli Crooks Strain," *Sensors 2020, Vol. 20, Page 4421*, vol. 20, no. 16, p. 4421, doi: 10.3390/S20164421.

[6] M. Xu *et al.*, (2022) "A Promising Crystalline KCl: Electrolyte Material for Studying the Electrochemical Properties of Cerium on Liquid Indium Electrodes," *Crystals 2022, Vol. 12, Page 1509*, vol. 12, no. 11, p. 1509, doi: 10.3390/CRYST12111509.

[7] P. Ramiah Rajasekaran, A. A. Chapin, D. N. Quan, J. Herberholz, W. E. Bentley, and R. Ghodssi, (2020) "3D-Printed electrochemical sensor-integrated transwell systems," *Microsystems & Nanoengineering 2020 6:1*, vol. 6, no. 1, pp. 1–12, doi: 10.1038/s41378-020-00208-z.

[8] C. Miller and B. A. Patel, (2024) "Creative design in fused filament fabrication 3D-Printed electrochemical sensors for detection of biomolecules," *TrAC Trends in Analytical Chemistry*, vol. 179, p. 117868, doi: 10.1016/J.TRAC.2024.117868.

[9] J. Hall, A. Tanner, and A. Eldek, (2023) "Remote Hands-on Experience for Students in Undergraduate Computer and Electrical Engineering," *J Syst Cybern Inf*, vol. 21, no. 1, pp. 47–53, doi: 10.54808/JSCI.21.01.47.

[10] R. Domingo-Roca, A. R. Macdonald, S. Hannah, and D. K. Corrigan, (2022) "Integrated multi-material portable 3D-printed platform for electrochemical detection of dopamine and glucose," *Analyst*, vol. 147, no. 20, pp. 4598–4606, doi: 10.1039/D2AN00862A.

[11] Z. Ma, J. Wang, L. Qin, and A. Chortos, (2024) "3D printing in biofabrication: From surface textures to biological engineering," *Chemical Engineering Journal*, vol. 500, p. 156477, doi: 10.1016/J.CEJ.2024.156477.

[12] J. Hussan K S *et al.*, (2024) "Fabrication and challenges of 3D printed sensors for biomedical applications-Comprehensive review," *Results in Engineering*, vol. 21, p. 101867, doi: 10.1016/J.RINENG.2024.101867.

[13] G. Remaggi, A. Zaccarelli, and L. Elviri, (2022) "3D Printing Technologies in Biosensors Production: Recent Developments," *Chemosensors*, vol. 10, no. 2, p. 65, doi: 10.3390/CHEMOSENSORS10020065/S1.